Low-Overhead Near-Field Beam Training Based on Bayesian Regression

Zhuo Xu, Zijian Zhang, *Graduate Student Member, IEEE*, and Linglong Dai, *Fellow, IEEE*
Department of Electronic Engineering, Tsinghua University,
State Key Laboratory of Space Network and Communications, Beijing 100084, China
Email: xz23@mails.tsinghua.edu.cn, zhangzj20@mails.tsinghua.edu.cn, daill@tsinghua.edu.cn

ICC 2025 - IEEE International Conference on Communications | 979-8-3315-0521-9/25/$31.00 ©2025 IEEE | DOI: 10.1109/ICC52391.2025.11161432

***Abstract*—In extremely large-scale multiple input multiple output (XL-MIMO) systems, near-field beam training is an essential way to acquire channel state information. To reduce the high training overhead brought by the additional distance dimension of the near-field codebook, some overhead-reduced near-field beam training schemes were proposed in the literature. However, existing schemes ignore the correlation between different near-field beams. In this paper, we propose a Bayesian regression-based near-field beam training scheme, which fully utilizes the correlation between near-field codewords to reduce the training overhead. Specifically, inspired by Bayesian regression, we model the received signal corresponding to different near-field codewords as a Gaussian process and determine the optimal codeword by iteratively updating the posterior distribution and designing the codeword searching order. Besides, different searching strategies are analysed and compared. The proposed scheme only requires searching for a few codewords instead of the entire codebook, which reduces the high training overhead. Simulation results verify the effectiveness of the proposed Bayesian regression-based near-field beam training scheme, which significantly reduces the training overhead while maintaining the high achievable rate performance.**

***Index Terms*—Beam training, extremely large-scale MIMO (XL-MIMO), near-field, Bayesian regression.**

I. Introduction

In recent years, the extremely large-scale MIMO (XL-MIMO) has been considered as one of the potential key technologies in the sixth-generation (6G) communications [1]. To fully utilize the high multiplexing gain in XL-MIMO systems, obtaining precise channel state information (CSI) is especially crucial and beam training is an efficient way, which searches codewords from a predefined codebook and selects the optimal codeword [2].

However, in XL-MIMO systems, beam training will face the challenge of additional high training overhead. Specifically, with the increasing number of the array antennas causing the enlargement of the near-field region, the near-field region should be accurately modeled by the spherical-wave model rather than the planar-wave model applied in far-field [3]. Unlike the far-field channel only determined by the angle, the near-field channel is related to both angle and distance. Accordingly, the near-field polar-domain codebook is proposed in [4], where each codeword corresponds to a near-field beam which could focus the beam on specific locations. Compared to the far-field DFT codebook, the near-field polar-domain codebook considers additional distance dimension so its size is the product of the number of angle and distance sampling grids. Therefore, it will bring extremely huge training overhead if the exhaustive searching is performed.

To reduce the high training overhead of the exhaustive searching scheme, several low-overhead near-field beam training schemes have been proposed. For example, a two-phase near-field beam training scheme is proposed in [5], where in the first phase the angle is searched and selected through the DFT codebook and the distance is determined in the second phase. Besides, some near-field hierarchical beam training schemes are proposed [6], [7]. Specifically, it is performed through the hierarchical codebook with different spatial resolution, where the resolution gradually increases as the searching range gradually decreases. In addition, artificial intelligence (AI) technologies such as neural networks and contrastive learning are also applied in near-field beam training to reduce the training overhead [8], [9].

However, the above near-field beam training methods usually overlooked the correlation between different near-field beams. Specifically, the received signal corresponding to different near-field beams is highly correlated. In other words, the measured received signal can not only provide the information about its corresponding codeword, but also the other codewords. Consequently, how to fully utilize the correlation between near-field codewords to reduce the overhead of near-field beam training is a critical problem.

To solve this problem, in this paper, we first apply Bayesian regression [10] into near-field beam training and propose a near-field Bayesian regression-based beam training (BRBT) scheme, where the optimal near-field codeword can be determined by searching only a small number of codewords. Specifically, we set the received signal corresponding to different codewords as the objective function in Bayesian regression and model the problem of selecting the optimal codeword in near-field beam training problem as finding the maximum value point of the posterior mean of the reconstructed objective function in Bayesian regression. During the entire process, the base station (BS) transmits the pilot signal to the user and iteratively update the posterior mean, covariance and variance according to the received signal from user's feedback. In each iteration, the next searching codeword is determined by maximizing the acquisition function corresponding to different searching strategies. After completing multiple iterations of searching, the optimal codeword is determined. Besides, we analyse and

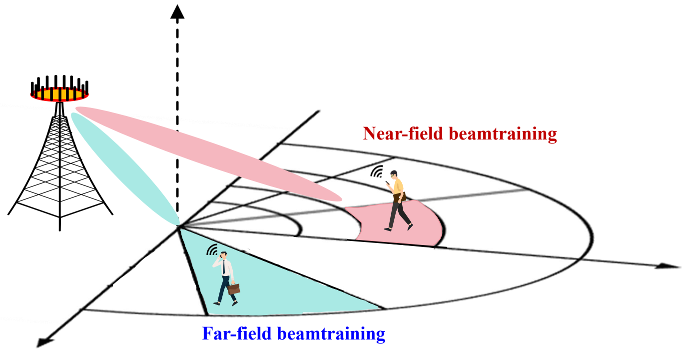

Fig. 1. Illustration of near-field beam training in XL-MIMO systems.

compare different searching strategies, which are particularly important for the overall performance of the proposed scheme. Simulation results demonstrate the superiority of the proposed BRBT scheme, which can achieve nearly-optimal achievable rate performance with low training overhead.

II. System Model

A. Signal Model and Channel Model

As shown in Fig. 1, the single-cell downlink XL-MIMO communication systems is considered, where the BS is equipped with a N-element uniform linear array (ULA) and serves one user with single-antenna. Without loss of generality, we adopt the fully-digital precoding structure, where each antenna is equipped with one RF chain, i.e., $N_{\mathrm{RF}} = N$. The fully-digital precoding structure can be easily extended to hybrid precoding structure.

Let $\mathbf{h} \in \mathbb{C}^{N\times 1}$ denotes downlink channel between the BS and the user, and the received signal y can be expressed as

$$y = \mathbf{h}^H \mathbf{w} s + n, \tag{1}$$

where $\mathbf{w} \in \mathbb{C}^{N\times 1}$ denotes the transmit beamforming vector, s denotes the power-normalized transmitted signal and n denotes the received noise following the distribution $\mathcal{CN}\left(0, \sigma^2\right)$. It should be emphasized that since the channel $\mathbf{h}$ is generally dominated by the main path, we only need to search the physical direction of the main path by beam training [6]. Therefore, in this paper only the main path is considered.

Generally, the channel model can be divided into the far-field channel model and the near-field channel model by the electromagnetic wave propagation characteristics. In the XL-MIMO systems, the spherical-wave model should be used to characterize the near-field channel. According to the widely-adopted Saleh-Valenzuela channel model, the near-field channel $\mathbf{h}$ can be expressed as [4]

$$\mathbf{h} = \sqrt{N}\alpha \mathbf{b}(\theta, r), \tag{2}$$

where α denotes the complex path gain of the line-of-sight (LoS) path, $\mathbf{b}(\theta, r)$ denotes the near-field beam steering vector and $\theta \in [-1, 1]$ denotes the spatial direction. Different from the far-field beam steering vector focusing the beam energy towards a specific direction, the near-field beam steering vector is able to focus the beam energy on a specific location. So the near-field beam steering vector is also called the near-field beam focusing vector. For the ULA, the near-field beam focusing vector $\mathbf{b}(\theta, r)$ can be expressed as

$$\mathbf{b}(\theta, r) = \frac{1}{\sqrt{N}}\left[e^{-jk(r^{(0)}-r)}, \cdots, e^{-jk(r^{(N-1)}-r)}\right]^T, \tag{3}$$

where $k = \frac{2\pi}{\lambda}$ is the wavenumber, $r^{(n)}$ denotes the distance between the user and the nth BS antenna element and r denotes the distance between the user and the center of the BS antenna. The distance $r^{(n)}$ can be written as

$$\begin{aligned} r^{(n)} &= \sqrt{r^2 - 2ndr\theta + n^2 d^2} \\ &\overset{(a)}{\approx} r - nd\theta + \frac{n^2 d^2}{2r}(1-\theta^2), \end{aligned} \tag{4}$$

where approximation (a) is the Fresnel approximation, which is derived by the second-order Taylor expansion $\sqrt{1+x} = 1 + \frac{x}{2} - \frac{x^2}{8} + \mathcal{O}(x^2)$. It can be obtained from (2) and (3) that the near-field channel is not only related to the angle of the user, but also to the distance between the user and the BS. Before the downlink date transmission, the BS should perform the beam training procedure to ensure that the beam to be transmitted aligns with the main path.

B. Near-field Beam Training

For the given beamforming vector $\mathbf{w}$, the achievable rate R of the user can be expressed as

$$R = \log_2\left(1 + \frac{|\mathbf{h}^H \mathbf{w}|^2}{\sigma^2}\right). \tag{5}$$

The main purpose of the near-field beam training is to select the optimal codeword from the predefined codebook to maximize the achievable rate R. The near-field beam training problem can be formulated as

$$\mathbf{w}^* = \arg\max_{\mathbf{w}\in\mathcal{W}} R, \tag{6}$$

where $\mathcal{W}$ denotes the predefined near-field codebook. According to Algorithm 1 in [4], the near-field polar-domain codebook can be represented as

$$\mathcal{W} = [\mathbf{b}(\theta_1, r_1^1), \cdots, \mathbf{b}(\theta_1, r_1^{S_1}), \cdots, \mathbf{b}(\theta_N, r_N^{S_N})], \tag{7}$$

where each column of the codebook $\mathcal{W}$ corresponds the codeword focusing on a specific position, and S_n denotes the number of sampled distances at the specific angle θ_n. As illustrated in Fig. 1, different from the far-field beam training only searching the angle of the user, the near-field beam training searches both the angle and the distance. One easy way to solve the near-field beam training problem (6) is exhaustive searching scheme. However, due to the additional distance dimension, the training overhead of the exhaustive searching scheme is the product of angle samples and distance samples, i.e., $|\mathcal{W}| = N\sum_{n=1}^{N} S_n$. This high training overhead is unacceptable in practical XL-MIMO systems. Therefore, low-overhead near-field beam training schemes are needed and our proposed Bayesian regression-based near-field beam training scheme will be introduced in the following section.

III. Proposed Bayesian Regression-Based Beam Training Scheme

In this section, we introduce the preliminary knowledge of Bayesian regression, proposed the BRBT scheme and compare different searching strategies of the proposed scheme.

A. Preliminary Knowledge of Bayesian Regression

To recover the objective function $f(\mathbf{x})$ only from few samples, Bayesian regression is widely considered an efficient solution, which can design the sampling order and recover $f(\mathbf{x})$ via its experiential kernels [10]. Specifically, the objective function $f(\mathbf{x})$ can be modeled as a Gaussian stochastic process $\mathcal{GP}\left(\mu\left(\mathbf{x}\right), k\left(\mathbf{x}, \mathbf{x}'\right)\right)$, where any stochastic process with finite dimensions follows the consistent multivariate Gaussian distribution [11]. It is completely determined by the mean function $\mu\left(\mathbf{x}\right)$ and covariance kernel $k\left(\mathbf{x}, \mathbf{x}'\right)$. Without loss of generality, the squared exponential kernel is considered in this paper, which can be expressed as

$$k(\mathbf{x}, \mathbf{x}') = \alpha^2 e^{-\frac{\|\mathbf{x}-\mathbf{x}'\|^2}{\eta^2}}, \tag{8}$$

where α and η are adjustable hyperparameters. Based on (8), the kernel matrix $\mathbf{K}$ can be expressed as

$$\mathbf{K} = \begin{bmatrix} k(\mathbf{x}^1, \mathbf{x}^1) & \cdots & k(\mathbf{x}^1, \mathbf{x}^m) \\ \vdots & \ddots & \vdots \\ k(\mathbf{x}^m, \mathbf{x}^1) & \cdots & k(\mathbf{x}^m, \mathbf{x}^m) \end{bmatrix}. \tag{9}$$

After determining the kernel function, let $\mathbf{y}^t = [y^1, \cdots, y^t]^{\mathrm{T}}$ denote t measurements for samples in $\mathcal{S}^t = \{\mathbf{x}^1, \cdots, \mathbf{x}^t\}$, where $y^i = f(\mathbf{x}^i) + n_i$ and n_i denotes the noise following $n_i \sim \mathcal{CN}\left(0, \delta^2\right)$. The objective function $f(\mathbf{x})$ and measurements $\mathbf{y}^t$ follow the joint Gaussian distribution, which can be expressed as

$$\begin{bmatrix} f\left(\mathbf{x}\right) \\ \mathbf{y}^t \end{bmatrix} \sim \mathcal{CN}\left(\begin{bmatrix} \mu\left(\mathbf{x}\right) \\ \boldsymbol{\mu}^t \end{bmatrix}, \begin{bmatrix} k\left(\mathbf{x}, \mathbf{x}'\right) & (\mathbf{k}^t(\mathbf{x}))^{\mathrm{H}} \\ \mathbf{k}^t(\mathbf{x}) & \mathbf{K}^t + \delta^2 \mathbf{I}_t \end{bmatrix} \right), \tag{10}$$

where $\mathbf{k}^t = \left[k\left(\mathbf{x}^1, \mathbf{x}\right), \cdots, k\left(\mathbf{x}^t, \mathbf{x}\right)\right]^{\mathrm{T}}$ and $\boldsymbol{\mu}^t = \left[\mu\left(\mathbf{x}^1\right), \cdots, \mu\left(\mathbf{x}^t\right)\right]^{\mathrm{T}}$. For given $\mathbf{y}^t$, the posterior distribution of $f(\mathbf{x})$ is also a Gaussian process, and its posterior mean, covariance and variance can be expressed as

$$\mu^t\left(\mathbf{x}\right) = \mu\left(\mathbf{x}\right) + \left(\mathbf{k}^t(\mathbf{x})\right)^{\mathrm{H}} \left(\mathbf{K}^t + \delta^2 \mathbf{I}_t\right)^{-1} \left(\mathbf{y}^t - \boldsymbol{\mu}^t\right), \tag{11}$$

$$k^t\left(\mathbf{x}, \mathbf{x}'\right) = k\left(\mathbf{x}, \mathbf{x}'\right) - \left(\mathbf{k}^t(\mathbf{x})\right)^{\mathrm{H}} \left(\mathbf{K}^t + \delta^2 \mathbf{I}_t\right)^{-1} \mathbf{k}^t(\mathbf{x}), \tag{12}$$

$$\sigma^t(\mathbf{x}) = k^t\left(\mathbf{x}, \mathbf{x}\right). \tag{13}$$

Then, the sampling strategy can be formulated based on the posterior mean (11), covariance (12) and variance (13), so the next sampling point can be determined.

B. Proposed Bayesian Regression-based Beam Training

In near-field beam training problem, the received signal corresponding to different near-field codewords is highly correlated. Inspired by this, we model the problem of selecting the optimal codeword in near-field beam training problem as finding the maximum value point of the objective function in Bayesian regression and propose a novel near-field BRBT scheme. Specifically, for different codewords $\mathbf{w}_i$, where $i = 1, 2, \cdots, |\mathcal{W}|$, the noiseless received signal vector $\mathbf{g}$ can be expressed as

$$\mathbf{g} = \mathbf{h}^H \mathcal{W}, \tag{14}$$

where $\mathbf{g} \in \mathbb{C}^{1\times|\mathcal{W}|}$, $\mathcal{W} \in \mathbb{C}^{N\times|\mathcal{W}|}$ and $|\mathcal{W}|$ denotes the number of codewords in near-field polar-domain codebook as defined in (7). We can model $\mathbf{g}$ as a Gaussian progress $\mathcal{GP}\left(\mathbf{0}_N, \boldsymbol{\Sigma}\right)$, where $\Sigma \in \mathbb{C}^{|\mathcal{W}|\times|\mathcal{W}|}$ denotes the squared exponential kernel matrix, which can be expressed as

$$\boldsymbol{\Sigma}(i, j) = \alpha^2 e^{-\frac{\|\mathbf{w}_i - \mathbf{w}_j\|^2}{\eta^2}}, \tag{15}$$

where $i, j \in \{1, \cdots, |\mathcal{W}|\}$. Let Ω denotes the index of the previous searched codewords and $\mathbf{g}_\Omega \in \mathbb{C}^{\dim(\Omega)}$ denotes the corresponding received signal, where $\mathbf{g}_\Omega = \mathbf{g}\left(\Omega\right) + \mathbf{n}_\Omega$ with $\mathbf{n}_\Omega \sim \mathcal{CN}(\mathbf{0}_{\dim(\Omega)}, \sigma^2 \mathbf{I}_{\dim(\Omega)})$. Therefore, similar to (10), the joint distribution of $\mathbf{g}$ and $\mathbf{g}_\Omega$ can be expressed as

$$\begin{bmatrix} \mathbf{g} \\ \mathbf{g}_\Omega \end{bmatrix} \sim \mathcal{CN}\left(\begin{bmatrix} \mathbf{0}_N \\ \mathbf{0}_{\dim(\Omega)} \end{bmatrix}, \begin{bmatrix} \boldsymbol{\Sigma} & \boldsymbol{\Sigma}\left(:, \Omega\right) \\ \boldsymbol{\Sigma}\left(\Omega, :\right) & \boldsymbol{\Sigma}\left(\Omega, \Omega\right) + \sigma^2 \mathbf{I}_{\dim(\Omega)} \end{bmatrix} \right). \tag{16}$$

Thus, for given $\mathbf{g}_\Omega$, the posterior mean $\boldsymbol{\mu}_\Omega$, covariance $\boldsymbol{\Sigma}_\Omega$ and variance $\boldsymbol{\sigma}_\Omega$ can be obtained:

$$\boldsymbol{\mu}_\Omega = \boldsymbol{\Sigma}(:, \Omega) \left(\boldsymbol{\Sigma}(\Omega, \Omega) + \sigma^2 \mathbf{I}_{\dim(\Omega)}\right)^{-1} \mathbf{g}_\Omega, \tag{17}$$

$$\boldsymbol{\Sigma}_\Omega = \boldsymbol{\Sigma} - (\boldsymbol{\Sigma}(\Omega, :))^{\mathrm{H}} \left(\boldsymbol{\Sigma}(\Omega, \Omega) + \sigma^2 \mathbf{I}_{\dim(\Omega)}\right)^{-1} \boldsymbol{\Sigma}(\Omega, :), \tag{18}$$

$$\boldsymbol{\sigma}_\Omega = \boldsymbol{\Sigma}_\Omega(n, n). \tag{19}$$

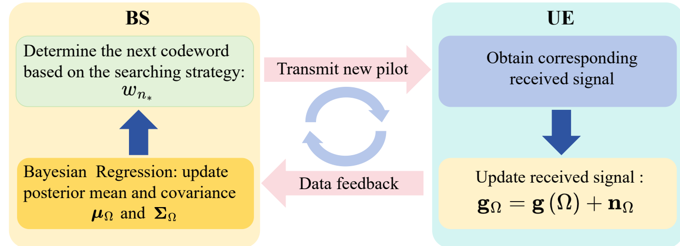

Fig. 2. A flowchart of the proposed Bayesian regression-based near-field beam training scheme.

To summarize, the flowchart and overall framework of the proposed Bayesian regression-based near-field beamtraining scheme is shown in Fig. 2 and **Algorithm 1**, respectively. Specifically, the BS selects the codeword and transmits the corresponding pilot signal to the user. Then, the user updates the received signal $\mathbf{g}_\Omega$ and reports the data feedback to the BS. It should be noted that the feedback data in the proposed scheme is the actual value not a binary sequence. Next, the BS can update the posterior mean $\boldsymbol{\mu}_\Omega$, covariance $\boldsymbol{\Sigma}_\Omega$, variance $\boldsymbol{\sigma}_\Omega$ and determine the next codeword based on the searching strategy. Specifically, different searching strategies correspond to different acquisition functions $V(\boldsymbol{x})$, which determine the searching order of codewords and the accuracy of the posterior predictive distribution in Bayesian regression [12]. In each iteration, the acquisition function is maximized to determine the next codeword, the Gaussian process is updated and the process is iterated. It should be emphasized that selecting the appropriate searching strategy is particularly important for the overall performance of the proposed scheme, which will be discussed in the following subsection.

Algorithm 1 Overall Framework of the proposed BRBT

Inputs: Near-field polar-domain codebook $\mathcal{W}$, kernal matrix $\mathbf{\Sigma}$, number of pilots $T_{\max}$.

Output: Optimal codeword $\mathbf{w}^*$.

```
Initialization: Ω = ∅.
for t = 1, 2, ···, T_max do
    Received signal power update: g_Ω = g(Ω) + n_Ω.
    Posterior mean μ_Ω, covariance Σ_Ω and variance σ_Ω update according to (17), (18) and (19).
    Determine the next codeword by maximizing the acquisition function V(x) according to the searching strategy: x_{t+1} = argmax_{x∈Ω_t} V(x).
    Index of searched codewords update: Ω_t ∪ x_{t+1}.
end for
Determine the index of the optimal codeword based on the maximum point of μ_Ω and select the corresponding codeword as the optimal codeword w*.
return Optimal codeword w*.
```

C. Comparison between Different Searching Strategies

As discussed before, the searching strategy is the key factor affecting the performance of the proposed scheme. In this subsection, different searching strategies of the proposed BRBT scheme are analysed and compared.

1) Exploitation-based Strategy: The goal of near-field beam training is to select the optimal codeword which maximizes the user's received signal power. In other words, we only need to determine the maximum value point of the posterior mean of the reconstructed objective function $\mathbf{g}_\Omega$ and select its corresponding codeword without accurately reconstructing the entire objective function [10]. Thus, the exploitation-based searching strategy can be directly applied, which tends to search the regions of the objective function likely to provide improvement based on the current best searching result.

Without loss of generality, we define $\mathbf{G}_{\Omega_T} = [\mathbf{g}_{\Omega_1}, \mathbf{g}_{\Omega_2}, \cdots, \mathbf{g}_{\Omega_T}]$, where $\mathbf{g}_{\Omega_t} = \mathbf{g}(\mathbf{w}_t) + n_t$, $n_t \sim \mathcal{CN}\left(0, \delta^2\right)$, $\mathbf{w}_t$ denotes the selected codeword at timeslot t and $T < |\mathcal{W}|$. For simplicity, we use $\boldsymbol{x}_t$ to represent $\mathbf{w}_t$. For the exploitation-based searching strategy, we should search points where the posterior mean is largest and the acquisition function $V^{\text{exploit}}(\boldsymbol{x})$ can be expressed as

$$V^{\text{exploit}}(\boldsymbol{x}) = \mu_{\boldsymbol{x}}. \tag{20}$$

Therefore, the exploitation-based searching strategy can be expressed as

$$\boldsymbol{x}_{t+1} = \underset{\boldsymbol{x}\in\Omega_t}{\operatorname{argmax}}\ V_t^{\text{exploit}}(\boldsymbol{x}) = \underset{\boldsymbol{x}\in\Omega_t}{\operatorname{argmax}}\ \mu_t(\boldsymbol{x}), \tag{21}$$

where $\Omega_t = \{\boldsymbol{x}_1, \ldots, \boldsymbol{x}_t\}$. Subsequently, we can update Ω_t by $\Omega_t \cup \boldsymbol{x}_{t+1}$, iterate the above process and select the optimal codeword. The main strength of this searching strategy is that it may obtain the extreme point quickly. However, it may face the risk of plunging into a local optimal solution, which seriously affects the overall performance of the BRBT scheme.

2) Exploration-based Strategy: Another method to select the optimal codeword is to first reconstruct the objective function globally well, then determine the estimated maximum value point of the posterior mean of the objective function and choose its corresponding codeword [13]. Thus, the exploration-based searching strategy can be applied, which tends to search the regions of high uncertainty. In other words, its goal is to reconstruct the entire unknown objective function as accurately and quickly as possible.

Specifically, to reduce the uncertainty of the estimated objective function, the main objective is to maximize the mutual information (or the information gain) between $\mathbf{g}$ and $\mathbf{g}_\Omega$, which can be expressed as

$$\begin{aligned} \max I(\mathbf{g}_\Omega; \mathbf{g}) &= \mathrm{H}(\mathbf{g}_\Omega) - \mathrm{H}(\mathbf{g}_\Omega|\mathbf{g}) \\ &= \log\left|\mathbf{I}_{\dim(\Omega)} + \frac{1}{\sigma^2}\mathbf{\Sigma}_\Omega\right|, \end{aligned} \tag{22}$$

where $\mathrm{H}(\cdot)$ denotes the entropy and for a Gaussian distribution, $\mathrm{H}(N(\mu,\Sigma)) = \frac{1}{2}\log|2\pi e\Sigma|$. However, solving the problem (22) is NP-hard. It can be approximated by an efficient greedy algorithm based on Gaussian process regression (GPR) [13]. Specifically, we set $F(\Omega) = I(\mathbf{g}_\Omega; \mathbf{g})$ and set the posterior variance as the acquisition function, i.e.,

$$V^{\text{explore}}(\boldsymbol{x}) = \boldsymbol{\sigma}_{\boldsymbol{x}}. \tag{23}$$

Therefore, the exploration-based searching strategy can be expressed as

$$\boldsymbol{x}_{t+1} = \underset{\boldsymbol{x}\in\Omega_t}{\operatorname{argmax}}\ V_t^{\text{explore}}(\boldsymbol{x}) = \underset{\boldsymbol{x}\in\Omega_t}{\operatorname{argmax}}\ \sigma_t(\boldsymbol{x}), \tag{24}$$

where $\Omega_t = \{\boldsymbol{x}_1, \ldots, \boldsymbol{x}_t\}$. Besides, this strategy can guarantee at least a constant fraction of the optimal information gain after T rounds of searching [13], i.e.,

$$F(\Omega_T) \geq (1 - \frac{1}{e}) \max_{|\Omega|\leq T} F(\Omega), \tag{25}$$

where $\Omega_T = \{\boldsymbol{x}_1, \ldots, \boldsymbol{x}_T\}$. The main strength of this exploration-based strategy is that it can reconstruct the entire objective function accurately and quickly by gradually reducing the uncertainty which prevents plunging into a local optimal solution. However, it may search for many "worthless points" and increase searching overhead.

3) Exploration-exploitation Balanced Strategy: Based on the above analysis, a exploration-exploitation balanced strategy should be adopted, which can dynamically trade off between bringing performance improvement and reducing uncertainty when determining the next codeword. Thus, corresponding acquisition function $V^{\text{balanced}}(\boldsymbol{x})$ of the exploration-exploitation balanced strategy should be determined and three effective functions are discussed as follows.

A) Probability of improvement (PI): A typical acquisition function of this strategy is called *probability of improvement* [10], which can be expressed as

$$\begin{aligned}\mathrm{PI}(\boldsymbol{x}) &= P(\mathbf{g}(\boldsymbol{x}) \geq \mathbf{g}(\boldsymbol{x}^+) + \xi) \\ &= \Phi\left(\frac{\mu_{\boldsymbol{x}} - \mathbf{g}(\boldsymbol{x}^+) - \xi}{\boldsymbol{\sigma}_{\boldsymbol{x}}}\right),\end{aligned} \tag{26}$$

where $\Phi(\cdot)$ denotes the normal cumulative distribution function (CDF), $\mathbf{g}(\boldsymbol{x}^+) = \underset{\boldsymbol{x}_i \in \Omega_t}{\operatorname{argmax}}\ \mathbf{g}(\boldsymbol{x}_i)$, and ξ denotes the adjustable parameter. It is recommended in that ξ should decrease gradually throughout the entire search process. Specifically, when ξ is enough high early, it tends to search the regions of high uncertainty and the exploration-based strategy dominates. When ξ becomes 0, the exploration-exploitation balanced strategy is transformed into the exploitation-based strategy.

B) Expected improvement (EI): Another acquisition function of the exploration-exploitation balanced strategy is *expected improvement*, which considers both the probability and degree of the improvement [10]. Specifically, the *expected improvement* acquisition function can be expressed as

$$\mathrm{EI}(\boldsymbol{x}) = \begin{cases}(\mu_{\boldsymbol{x}} - \mathbf{g}(\boldsymbol{x}^+) - \xi)\Phi(Z) + \boldsymbol{\sigma}_{\boldsymbol{x}}\phi(Z), & \boldsymbol{\sigma}_{\boldsymbol{x}} > 0 \\ 0, & \boldsymbol{\sigma}_{\boldsymbol{x}} = 0,\end{cases} \tag{27}$$

where

$$Z = \begin{cases}\frac{\mu_{\boldsymbol{x}} - \mathbf{g}(\boldsymbol{x}^+) - \xi}{\boldsymbol{\sigma}_{\boldsymbol{x}}}, & \boldsymbol{\sigma}_{\boldsymbol{x}} > 0 \\ 0, & \boldsymbol{\sigma}_{\boldsymbol{x}} = 0,\end{cases} \tag{28}$$

$\phi(\cdot)$ and $\Phi(\cdot)$ denote the probability density function (PDF) and CDF of the standard normal distribution and ξ is the adjustable parameter like in (26).

C) Gaussian process upper confidence bound (GP-UCB): Additionally, Gaussian process upper confidence bound is widely used as the acquisition function, which measures the quality of the codeword searching by quantifying regret [13]. Specifically, the goal of BRBT can be expressed as

$$\boldsymbol{x}^* = \underset{\boldsymbol{x} \in \mathcal{W}}{\operatorname{argmax}}\ \mathbf{g}(\boldsymbol{x}), \tag{29}$$

where $\boldsymbol{x}^*$ denotes the optimal codeword. One equivalent method for (29) is to minimize the cumulative regret, which can be expressed as

$$R_T = \sum_{t=1}^{T} r_t, \tag{30}$$

where $r_t = \mathbf{g}(\boldsymbol{x}^*) - \mathbf{g}(\boldsymbol{x}_t)$. However, solving (29) or minimizing the R_T is NP-hard. Thus, GP-UCB can be applied as the acquisition function, which can be expressed as

$$\text{GP–UCB}(\boldsymbol{x}) = \mu_{t-1}(\boldsymbol{x}) + \sqrt{\beta}_t \sigma_{t-1}(\boldsymbol{x}), \tag{31}$$

where β_t is a adjustable hyperparameter, which balances exploration and exploitation. Besides, β_t is usually set as: $\beta_t = 2\log(|\mathcal{W}|t^2\pi^2/6\delta)$, where $\delta \in (0,1)$. Different from the classical multi-armed bandit problem, the regrets of the GP-UCB algorithm is highly correlated to the kernel matrix $\mathbf{\Sigma}$. It has be proven in [13] that the cumulative regret of GP-UCB algorithm is bounded and sublinear for T with high probability, which means each round of regret could gradually decrease to choose the better point, i.e., $\lim_{T\to\infty} \frac{R_T}{T} = 0$.

For the computational complexity of the GP-UCB algorithm, it is mainly composed of the iterative update of GP–UCB$(\boldsymbol{x})$ and selecting optimal codeword after the iteration. Specifically, for the iterative update of GP–UCB$(\boldsymbol{x})$, its computational complexity is $\mathcal{O}\left(T^2\left(T^2 + |\mathcal{W}|T + |\mathcal{W}|^2\right)\right)$, according to (18) and (31). For selecting optimal codeword after the iteration, the computational complexity is $\mathcal{O}(|\mathcal{W}|)$.

IV. Simulation Results

In this section, simulation results are carried out to verify the performance of the proposed near-field BRBT scheme. The number of the BS antennas is $N = 256$, the carrier frequency is 30 GHz and the spacing between array elements is $d = \frac{\lambda}{2} = 0.5$ cm. For simplicity, we consider the single-user beam training scenario and the user is randomly distributed in a sector, where the spatial angle range and distance range are $[-\frac{\pi}{3}, \frac{\pi}{3}]$ and $[4\text{ m}, 80\text{ m}]$, respectively. The complex path gain of the LoS path is $\alpha \sim \mathcal{CN}(0,1)$. Moreover, for the proposed near-field BRBT scheme, we set the hyperparameters of the squared exponential kernel as $\alpha^2 = 1$ and $\eta^2 = \frac{2}{\Delta_{\text{index}}}$, where $\Delta_{\text{index}} = \sqrt{\Delta_\theta^2 + \frac{1}{\Delta_r^2}}$, Δ_θ and Δ_r denote the angle and distance sampling steps of the near-field codebook. Without loss of generality, in this paper we adopt the exploration-exploitation balanced strategy and select GP-UCB as the acquisition function for the proposed near-field BRBT scheme and set $\delta = 0.1$ of β_t.

First, the achievable rate performance of different schemes against the beam training overhead is shown in Fig. 3, where SNR = 10 dB and the beam training overhead increases from 0 to 1280. It can be shown that the proposed near-field Bayesian regression-base beam training scheme only needs 50 overhead to almost achieve the performance of the near-field exhaustive searching scheme, which can reduce almost 96% of the overhead of the near-field exhaustive searching scheme. Specifically, for the near-field two-phase and hierarchical beam training scheme, their beam training overhead are still strongly related to the size of the codebook and are usually unacceptable when the size of the codebook in XL-MIMO systems is large. For our proposed scheme, it can perform well with low overhead. This is because it fully utilizes the correlation between different codewords and when the number of transmitting pilots increases, the reconstructed objective function in Bayesian regression becomes more accurate and the optimal codeword can be quickly determined.

Besides, the achievable rate performance of different schemes against the SNR is shown in Fig. 4. Specifically, it can be shown that the proposed scheme can almost achieve the performance of the near-field exhaustive searching scheme and outperform the near-field two-phase and hierarchical beam training scheme. For the near-field two-phase scheme in [5], as it applies DFT codebook in the first phase, the near-field *energy spread* effect affects the accurracy of angle searching

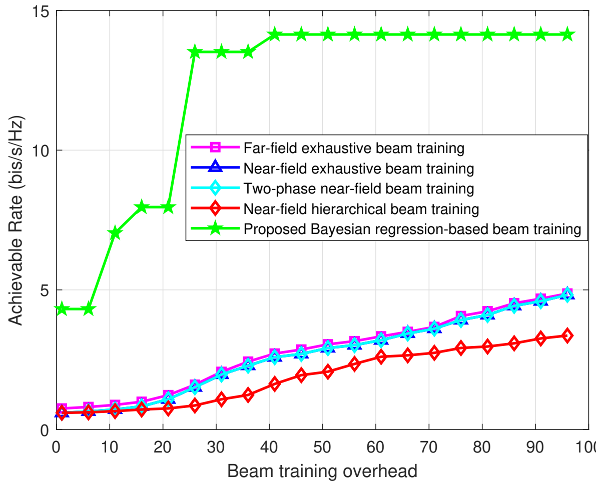

(a)

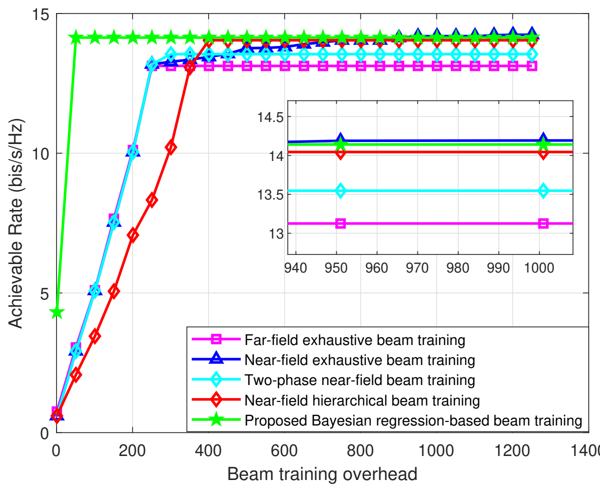

(b)

Fig. 3. Achievable rate performance vs. the beam training overhead.

and causes the performance loss. For the near-field hierarchical scheme in [6], as the wide beam is easily affected by noise, it faces the serious performance degradation at low SNR. The proposed scheme can exclude the influence of the above two factors and perform well.

V. Conclusions

In this paper, we first apply Bayesian regression into near-field beam training and propose a Bayesian regression-based near-field beam training scheme. Different from the existing near-field beam training schemes, the proposed scheme models the problem of selecting the optimal codeword in near-field beam training problem as finding the maximum value point of the posterior mean of the objective function in Bayesian regression, which fully utilized the correlation between near-field codewords to reduce the training overhead. Simulation results confirm that the efficiency of the proposed scheme, which only requires searching for a few codewords instead of the entire codebook to select the optimal codeword.

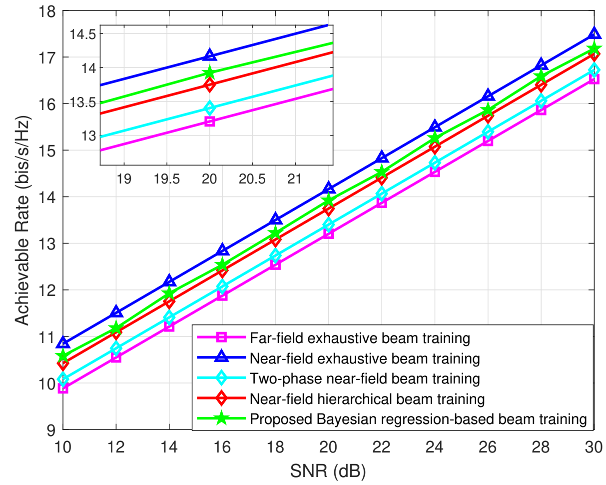

Fig. 4. Achievable rate performance vs. the SNR.

Acknowledgment

This work was funded by the National Science Fund for Distinguished Young Scholars (Grant No. 62325106).

References

[1] Z. Wang, J. Zhang, H. Du, D. Niyato, S. Cui, B. Ai, M. Debbah, K. B. Letaief, and H. V. Poor, "A tutorial on extremely large-scale MIMO for 6G: Fundamentals, signal processing, and applications," *IEEE Commun. Surv. Tutor.*, 2024.

[2] K. Chen, C. Qi, C.-X. Wang, and G. Y. Li, "Beam training and tracking for extremely large-scale MIMO communications," *IEEE Trans. Wireless Commun.*, vol. 23, no. 5, pp. 5048–5062, May 2024.

[3] M. Cui, Z. Wu, Y. Lu, X. Wei, and L. Dai, "Near-field MIMO communications for 6G: Fundamentals, challenges, potentials, and future directions," *IEEE Commun. Mag.*, vol. 61, no. 1, pp. 40–46, Jan. 2023.

[4] M. Cui and L. Dai, "Channel estimation for extremely large-scale MIMO: Far-field or near-field?" *IEEE Trans. Commun.*, vol. 70, no. 4, pp. 2663–2677, Apr. 2022.

[5] Y. Zhang, X. Wu, and C. You, "Fast near-field beam training for extremely large-scale array," *IEEE Wireless Commun. Lett.*, vol. 11, no. 12, pp. 2625–2629, Dec. 2022.

[6] Y. Lu, Z. Zhang, and L. Dai, "Hierarchical beam training for extremely large-scale MIMO: From far-field to near-field," *IEEE Trans. Commun.*, vol. 72, no. 4, pp. 2247–2259, Apr. 2024.

[7] X. Shi, J. Wang, Z. Sun, and J. Song, "Spatial-chirp codebook-based hierarchical beam training for extremely large-scale massive mimo," *IEEE Trans. Wireless Commun.*, vol. 23, no. 4, pp. 2824–2838, Aug. 2024.

[8] W. Liu, H. Ren, C. Pan, and J. Wang, "Deep learning based beam training for extremely large-scale massive MIMO in near-field domain," *IEEE Commun. Lett.*, vol. 27, no. 1, pp. 170–174, Jan. 2023.

[9] X. Zhang, H. Zhang, C. Li, Y. Huang, and L. Yang, "Environment-specific beam training for extremely large-scale MIMO systems via contrastive learning," *IEEE Commun. Lett.*, vol. 27, no. 10, pp. 2638–2642, Oct. 2023.

[10] E. Brochu, V. M. Cora, and N. De Freitas, "A tutorial on Bayesian optimization of expensive cost functions, with application to active user modeling and hierarchical reinforcement learning," *arXiv preprint arXiv:1012.2599*, 2010.

[11] Z. Zhang, J. Zhu, L. Dai, and R. Heath Jr, "Successive bayesian reconstructor for channel estimation in fluid antenna systems," *arXiv preprint arXiv:2312.06551*, 2024.

[12] S. Yang, B. Liu, Z. Hong, and Z. Zhang, "Bayesian optimization-based beam alignment for mmwave MIMO communication systems," in *2022 IEEE PIMRC*. IEEE, 2022, pp. 825–830.

[13] N. Srinivas, A. Krause, S. M. Kakade, and M. W. Seeger, "Information-theoretic regret bounds for gaussian process optimization in the bandit setting," *IEEE Trans. Inf. Theory*, vol. 58, no. 5, pp. 3250–3265, May 2012.